

Nuclear structure of ${}^5\text{H}$ in a three-body ${}^3\text{H}+n+n$ model

N. B. Shul'gina,^{1,2,*} B. V. Danilin,² L. V. Grigorenko,^{3,2} M. V. Zhukov,¹ and J. M. Bang⁴

¹*Department of Physics, Chalmers University of Technology and Göteborg University, S-41296 Göteborg, Sweden*

²*Russian Research Center "The Kurchatov Institute," 123182 Moscow, Russia*

³*Physics Department, University of Surrey, Guildford, Surrey GU2 5XH, England*

⁴*The Niels Bohr Institute, DK-2100 Copenhagen Ø, Denmark*

(Received 1 December 1999; published 20 June 2000)

Complete dynamical investigation of the extremely neutron-rich ${}^5\text{H}$ nucleus is performed in a three-body ${}^3\text{H}+n+n$ continuum. A three-body resonance enhancement is found for the "ground state" $J^\pi=1/2^+$ at about 2.5–3.0 MeV. The broad structures in the production cross sections correspond to wide $3/2^+$ and $5/2^+$ levels in the three-body continuum.

PACS number(s): 21.45.+v, 21.60.Cs, 27.10.+h

The ${}^5\text{H}$ nucleus belongs to the very neutron-rich nuclei beyond the neutron dripline. This nucleus has been studied theoretically [1,2], and experimentally [3–6] but until now the existence of the ${}^5\text{H}$ as a well-defined resonance still remains unclear. A lower limit on the mass of ${}^5\text{H}$ was obtained in [3] from the absence of sharp structures in the "mirror" ${}^3\text{He}({}^3\text{He},n){}^5\text{Be}$ reaction up to 4.2 MeV. This implies that ${}^5\text{H}$ is unbound by at least 2.1 MeV. According to [4] nothing except phase space, modified to account for possible dineutron decay was found in the pion absorption reactions ${}^6\text{Li}(\pi^-,p){}^5\text{H}$. However, in the ${}^7\text{Li}({}^6\text{Li},{}^8\text{B}){}^5\text{H}$ reaction [5] a resonance at about $E=5.2$ MeV, $\Gamma=4$ MeV was observed. The ${}^5\text{H}$ state with a resonance energy $E=7.4\pm 0.7$ MeV, $\Gamma=8\pm 3$ MeV was detected in ${}^9\text{Be}(\pi^-,pt){}^5\text{H}$ reaction [6]. Oscillator shell model calculations predict for the ${}^5\text{H}$ "ground state" $1/2^+$, $E=3.1$ MeV [1] and for the first "excited" states 5.54 MeV $5/2^+$, 7.39 MeV $3/2^+$, and 10.49 MeV $3/2^+$ [2] (E is the energy relative to the ${}^3\text{H}+n+n$ threshold). However, oscillator shell model calculations are valid only for narrow resonances and do not take into account the influence of continuum, which can lead, in principle, to complete dissolving of the possible states.

Qualitatively, if we neglect for a moment the spin of the ${}^3\text{H}$ core, ${}^5\text{H}$ could be considered as ${}^3\text{H}+2n$ in analogy with the neighboring neutron halo ${}^6\text{He}$ nucleus (${}^4\text{He}+2n$), since in both cases we have the s -wave Pauli repulsion in ${}^3\text{H}+n$ and ${}^4\text{He}+n$ subsystems and attraction in the p -wave. The ${}^3\text{H}+n$ interaction for the p -wave is weaker, than that for ${}^4\text{He}+n$ so we can expect the states analogous to 0^+ g.s. and 2^+ 1.8 MeV in ${}^6\text{He}$ to be lifted up in ${}^5\text{H}$ to continuum. Taking into account the spin of ${}^3\text{H}$ we can expect $1/2^+$ as a "ground state" and instead of 2^+ in ${}^6\text{He}$ we can expect the doublet $3/2^+$ and $5/2^+$, based on the same orbital configuration. Our previous calculations [7,8] of the ${}^6\text{He}$ ground state, the 2^+ resonance in ${}^6\text{He}$ and the 0^+ , 2^+ resonant states in ${}^6\text{Be}$ have demonstrated that mainly s - and p -wave interactions between clusters are responsible for the existence of those states. The same situation should be expected in the ${}^5\text{H}$ case.

This paper investigates this question within strict three-body ${}^3\text{H}+n+n$ dynamics with expansion on hyperspherical harmonics. This method provides the consistent solution of the bound state and three-body continuum problems for so called "democratic" systems, where none of the binary subsystems are bound [8].

The wave function (WF) is assumed to be a product of an inactive core part and the active three-body part. The latter is expanded on a generalized angle-spin basis

$$\Psi^{JM} = \sqrt{\frac{2}{\pi}} \frac{(2\pi)^3}{(\alpha\rho)^{5/2}} \sum_{K\gamma} i^K \left\{ \sum_{K'\gamma'} \chi_{K'\gamma'}^{K'\gamma'}(\alpha\rho) \mathcal{L}_{K'\gamma'}^{JM}(\Omega_\rho) \right\} \\ \times \sum_{M_L M_S} C_{LM_L M_S}^{JM} \mathcal{J}_{K_L I_x I_y}^{LM_L}(\Omega_\alpha), \\ \mathcal{L}_{K_L S_x I_x I_y}^{JM}(\Omega_\rho) = [\mathcal{J}_{K_L I_x I_y}^{LM_L}(\Omega_\rho) \otimes X_{S_x S_x}]_{JM},$$

where X_{S_x} is the coupled spin function of the two neutrons S_x and core $S_3=1/2$, while

$$\mathcal{J}_{K_L I_x I_y}^{LM_L}(\Omega_\rho) = \psi_K^{L I_x I_y}(\theta) [Y_{I_x}(\hat{x}) \otimes Y_{I_y}(\hat{y})]_{LM_L}$$

is a hyperspherical harmonic generated from a Jacobi polynomial in the hyperangle $\theta = \arctan(x/y)$. Here x and y are the absolute values of the normalized Jacobi coordinates $\mathbf{x} = \sqrt{1/2}\mathbf{r}_{nn}$ between neutrons and $\mathbf{y} = \sqrt{6/5}\mathbf{r}_{(nn)\text{core}}$ for the neutrons relative to the core. The hypermoment $K=L_x+L_y+2n$, ($n=0,1,\dots$), is the generalized angular momentum eigenvalue, related to the coordinate θ . Other quantum numbers are the Jacobi orbital momenta l_x and l_y and the total orbital momentum L . The three-body Schrödinger equation can be reduced to a two-body-like multichannel problem for the functions $\chi_{K'\gamma'}^{K'\gamma'}(\alpha\rho)$ in the hyperradius $\rho = \sqrt{x^2+y^2}$. Multi-index γ stands for the set of quantum numbers $\{L, S, S_x, l_x, l_y\}$. The wave number α is simply connected to the energy E and nucleon mass M : $\alpha^2 = 2ME$. The asymptotic behavior of the functions $\chi(\alpha\rho)$ at large ρ values is

$$\chi_{K'\gamma'}^{K'\gamma'}(\alpha\rho) \sim \delta_{K'\gamma'}^{K'\gamma'} \mathcal{H}_{\mathcal{L}}^-(\alpha\rho) - S_{K'\gamma'}^{K'\gamma'} \mathcal{H}_{\mathcal{L}}^+(\alpha\rho).$$

*Electronic address: shulgina@fy.chalmers.se

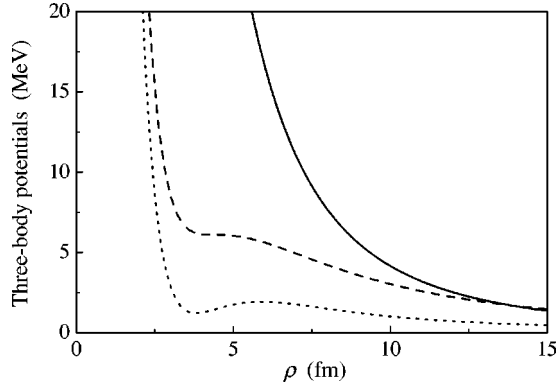


FIG. 1. Diagonal three-body potentials for the main resonating components of the WF: solid curve corresponds to $K=0, L=0, S=1/2, l_x=l_y=0$; dashed curve is $K=2, L=0, S=1/2, l_x=l_y=0$. There is pure repulsion in $K=0$, and no prominent pocket is seen in the $K=2$ potential. The attraction is provided by channel coupling as it can be seen in the main component of the *diagonalized* potential (dotted curve).

Here \mathcal{H}_L^\mp are the Riccati-Bessel functions of half-integer index $\mathcal{L}=K+3/2$, with asymptotics $\sim \exp(\mp i\kappa\rho)$, describing the in- and outgoing three-body spherical waves. $S_{K\gamma}^{K'\gamma'}$ is the S -matrix for the $3 \rightarrow 3$ scattering. Details of this representation and analysis of three-body continuum can be found in [7,8].

For the calculations we used the ${}^3\text{H}-n$ potential from [9], reproducing experimental ${}^3\text{H}-n$ and “mirror” ${}^3\text{He}-p$ scattering phases. This potential is based on scattering phases, obtained in [10], where the lowest broad 2^- resonance in the ${}^3\text{H}-n$ system is found at $E=3.4$ MeV above the ${}^3\text{H}-n$ threshold. More recently other experimental data [5,11] have appeared, where the spectrum of ${}^8\text{B}$ from the ${}^6\text{Li}({}^6\text{Li}, {}^8\text{B}){}^4\text{H}$ reaction at different projectile energies has been observed. As a result it was shown that ${}^4\text{H}$ is unstable in respect to the ${}^3\text{H}+n$ decay by 2.3 ± 0.3 MeV. An influence of these new data on our results is discussed below. The blocking of Pauli forbidden states was taken into account by a repulsive core in the s -wave potentials. The $n-n$ potential [12], including repulsion at small distances, as well as spin-orbit and tensor forces, was used in the calculations. We have performed our calculations with the restrictions $l_x < 4, l_y < 4$, and $K_{max} < 12$.

A sharp resonant (quasistationary) state should appear as a jump of 180° in the diagonal phase shifts. From the physical point of view the origin of quasistationary states is a pocket in one of the diagonal three-body potentials, which are a weighted sum of the pairwise interactions $\langle K\gamma | \sum_{ij} \hat{V}_{ij} | K\gamma \rangle$ and the three-body centrifugal barrier. The most important components of these potentials for the $1/2^+$ state are demonstrated in Fig. 1. One can see a rather shallow pocket in $K=2, L=0, S=1/2, S_x=0, l_x=0, l_y=0$ partial wave. This state carries presumably the quantum numbers of the ${}^3\text{H}+$ “dineutron.” The pocket for the ${}^5\text{H}$ $5/2^+$ state in $K=2, L=1, S=3/2, S_x=1, l_x=1, l_y=1$ partial wave is smaller. The pockets for other J^π states are completely absent. More shallow pockets for ${}^5\text{H}$ in comparison with 0^+

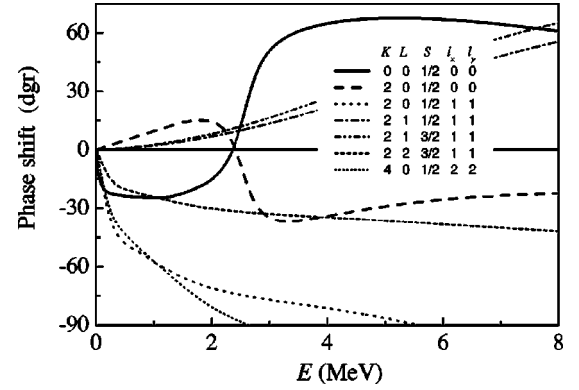


FIG. 2. Diagonal phase shifts for a few important components of the $1/2^+$ state WF. Components with $K=0, L=0, S=1/2, l_x=l_y=0$ (solid line) and $K=2, L=0, S=1/2, l_x=l_y=0$ (dashed line) have a resonance behavior.

and 2^+ in ${}^6\text{He}$ could have as a consequence that in ${}^5\text{H}$ we deal either with the top barrier resonances or with partial states spreading in continuum. The diagonal phase shifts of the $1/2^+$ continuum are shown in Fig. 2. The phase shifts show the resonant behavior in the dominating components of the WF around 2.5 MeV. Phase analysis of other J^π states have shown the absence of resonant behavior.

A measure of a continuum strength is the WF concentration in the interior region. It can be characterized by the sum of the diagonal interior norms:

$$N_{\rho_0}(E) = \frac{1}{\kappa^5} \sum_{K\gamma} \int_0^{\rho_0} d\rho |\chi_{K\gamma}^{K\gamma}(\kappa\rho)|^2. \quad (1)$$

The interior norm is a simplified measure of the overlap integrals in the transition amplitudes for various processes with three particles in the final state. We can choose $\rho_0 \sim 5-7$ fm, as the radius of the local maximum of the diagonal potential in a component $K\gamma$ with a pocket. For narrow resonances this prescription is very reliable: the energy dependence of $N(E)$ is exactly the same as the energy dependence of the cross sections. The interior norms for all J^π states in the continuum are shown in Fig. 3 (see also Table

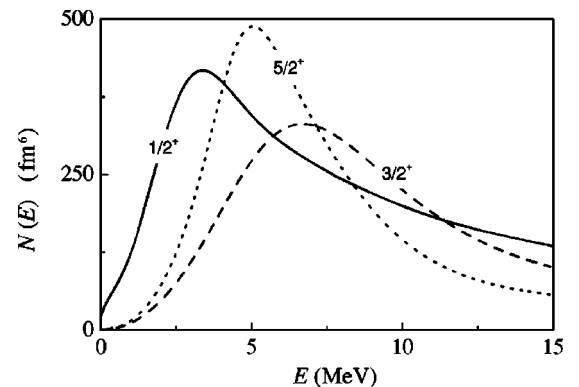


FIG. 3. Sum of the diagonal internal normalizations [see Eq. (1)] for $1/2^+, 3/2^+$, and $5/2^+$ states are shown by solid, dashed, and dotted lines, respectively.

TABLE I. Positions and widths of the states, obtained with a ${}^3\text{H}$ - n potential fitted to the data from [10]. The uncertainties are connected with different ways to define the properties of the wide states.

J^π	$1/2^+$	$3/2^+$	$5/2^+$
E (MeV)	2.5–3.0	6.4–6.9	4.6–5.0
Γ (MeV)	3–4	8	5

I). The $1/2^+$ strength peaks approximately 2.5 MeV above the threshold, the $5/2^+$ strength dominates between about 4 and 7 MeV with a peak at 5 MeV, the $3/2^+$ excitation shows a bump at about 7 MeV. Contrary to well-known resonances in ${}^6\text{He}$ and ${}^6\text{Be}$ where interior norms exhibit pronounced maxima [8] in almost all partial components, we have for the case of ${}^5\text{H}$ a complex interplay of the kinematic enhancement and a concentration of the strength due to the final-state interaction (FSI).

We can demonstrate that the valence neutrons in the ${}^5\text{H}$ are situated mainly outside of the ${}^3\text{H}$ core. Taking into account that the ${}^5\text{H}$ is a decaying state, in general the probability to find neutrons inside the ${}^3\text{H}$ core goes to zero. What we can do in this situation is to estimate the ratio, $N_3(E)/N_6(E)$, of norms Eq. (1) for regions ‘‘inside’’ and ‘‘outside’’ the core. The value $\rho_0 = 3$ fm is slightly larger, than the ρ value, corresponding to the case where the valence neutrons are situated on top of the ${}^3\text{H}$ core. We got the ratio near 0.03 for $E = 2.7$ MeV.

Although the interior norms, as functions of the energy, give us information about the positions and widths of the possible resonances, we would like to introduce a quantity which is more closely connected with the experimentally measured cross sections. The energy behavior of the missing mass (MM) cross section, which is measured in an experiment depends both on the initial and the final states:

$$d\sigma_{\text{MM}} \sim |\langle \Psi_f | \hat{V} | \Psi_i \rangle|^2 d\Omega_{\kappa} E^2 dE,$$

where $d\Omega_{\kappa} E^2 dE$ is a three-body phase space. The final-state WF Ψ_f is obtained as a result of our three-body calculations. The initial-state WF depends on the specific reaction where ${}^5\text{H}$ is produced. In a simple approximation the vertex for ${}^5\text{H}$ production can be simulated as

$$\hat{V} | \Psi_i \rangle = \sum_{K' \gamma'} \exp[-\rho/\rho_0] \mathcal{L}_{K' \gamma'}(\Omega_{\rho}),$$

where ‘‘reaction radius’’ ρ_0 can be taken in the interval 5–7 fm, the same as for the internal normalization. The initial-state WF simulated in this way takes into account the reaction volume and implies equal population of all sets with quantum numbers $K' \gamma'$ in the reaction process.

So, we estimated the energy dependence of the MM cross section as

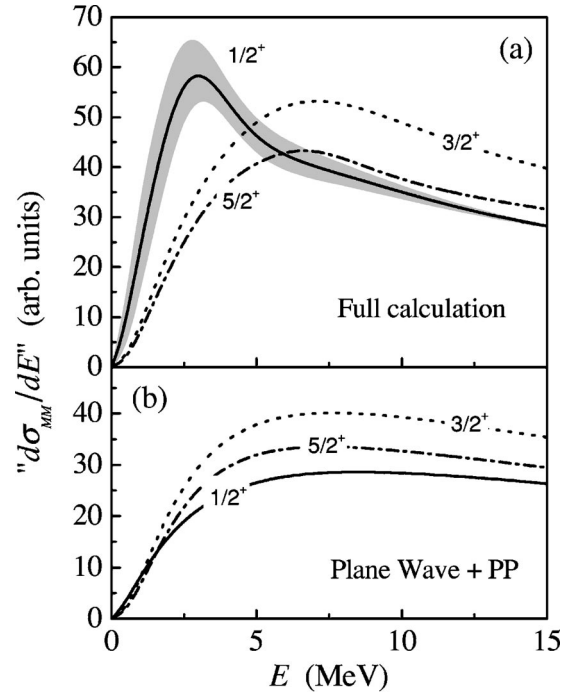


FIG. 4. Missing mass spectra for $1/2^+$, $3/2^+$, and $5/2^+$ states, evaluated by Eq. (2), are shown for $\rho_0 = 6$ fm by solid, dashed, and dotted lines in (a). The gray area around the solid curve shows the variation of the $1/2^+$ spectrum, when ρ_0 is varied between 5 and 7 fm. (b) shows the same as (a), but without FSI (except the s -wave core in the ${}^3\text{H}$ - n channel, accounting for the Pauli principle).

$$d\sigma_{\text{MM}} \sim \sum_{K\gamma} \left| \sum_{K'\gamma'} \int d\rho \chi_{K\gamma}^{K'\gamma'}(\kappa\rho) \exp[-\rho/\rho_0] \right|^2 \frac{dE}{\sqrt{E}}. \quad (2)$$

The results for $1/2^+$, $3/2^+$, $5/2^+$ states are shown in Fig. 4(a). While the $1/2^+$ state reveals itself as a relatively pronounced peak at about 2.5 MeV, the $3/2^+$ and $5/2^+$ excitations exhibit only broad structures. If all the states were equally populated in a reaction producing ${}^5\text{H}$, and if the energy resolution in an experiment were not high enough, the upper wide states could hamper the observation of the $1/2^+$ state. Probably, in the experiments [5,6] just the $3/2^+$, $5/2^+$ states, peaking at about 5–7 MeV, were observed.

Since the resonance we got for the $1/2^+$ state is relatively wide, we studied the sensitivity of the MM spectrum for the $1/2^+$ state to the ‘‘reaction radius’’ by varying ρ_0 within reasonable limits. The gray area around solid curve in Fig. 4(a) corresponds to ρ_0 varied between 5 and 7 fm. The sensitivity appears to be low: the resonance energy is shifted down by 0.3 MeV by increasing ρ_0 from 5 to 7 fm. This shift can be considered as an uncertainty of the model. Figure 4(b) gives the spectra obtained without the FSI for $\rho_0 = 6$ fm. By comparing the MM spectra with and without the FSI one can conclude that the $1/2^+$ state, being selectively excited, should be clearly seen above the ‘‘background.’’

An interesting problem arises when we wish to compare the spectra with and without final-state interactions. The problem is closely connected to the Pauli principle. If we

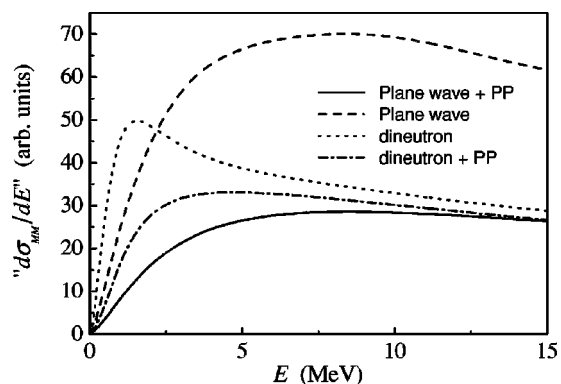


FIG. 5. Missing mass spectrum for the $1/2^+$ state without FSI. The solid line is the same as in Fig. 4(b); the dashed line indicates no FSI, no Pauli principle in any subsystem; the dotted line indicates the “dineutron” case: ${}^3\text{H}$ - n interaction is switched off in all partial waves; the dash-dotted line indicates the “dineutron” case but with the Pauli principle taken into account.

completely neglect the antisymmetrization of the wave function, obtained as a free solution of the three-body Schrödinger equation, we get a strong amplification of the spectrum, as is shown in Fig. 5, dashed line. The exact accounting for the Pauli principle in the two-neutron subsystem, and the approximate accounting by means of the repulsion in the s -wave ${}^3\text{He}$ - n subsystem, leads to considerable reduction of the spectrum (Fig. 5, solid line). The same situation takes place when one wants to describe the experimental spectrum of ${}^5\text{H}$ by means of two-body ${}^3\text{H}$ + “dineutron” decay, as it was done in Ref. [4]. We simulated this scenario by switching off the ${}^3\text{H}+n$ interaction (i) in all partial waves and (ii) in all partial waves except the repulsion in the s -wave, which accounts for the Pauli principle. The results (dotted and dash-dotted curves in Fig. 5) differ drastically. With the Pauli principle taken into account, the ${}^3\text{H}$ + “dineutron” scenario fails to describe the $1/2^+$ resonance.

A summary of the results is in Table I. For a $1/2^+$ excitation, the spectrum shows a maximum at 2.5 MeV. When

the experimental data from [11] are used instead of [10] to fit the ${}^3\text{H}$ - n interaction, the position of the $1/2^+$ state shifts down by 0.2–0.4 MeV. Diagonal phases reflect the resonant behavior in some partial components which corresponds to the top barrier resonance case. The width values shown in Table I were estimated as full widths at half maximum for internal norms or cross sections after subtraction of the contribution connected with the plane waves.¹ Wide bumps appear for $3/2^+$ and $5/2^+$ excitations with maxima very close to the positions given by the shell model [2]. Generally speaking, our three-cluster model is valid up to the ${}^3\text{H}$ breakup threshold (~ 6 MeV). However, we could not expect a large deviation of the calculated spectrum from the experimental one at higher energy if the ${}^3\text{H}$ cluster were observed in a final state. As for the experimental observation of the $1/2^+$ resonant excitation in the ${}^5\text{H}$ system, it would depend on the reaction mechanism, enhancing or suppressing the resonant partial waves. If angular distributions were measured, these partial waves could be separated.

A JINR-RIKEN-Kurchatov-GANIL experiment searching for ${}^5\text{H}$ in the reaction ${}^6\text{He}(p,2p){}^5\text{H}$ has been performed very recently in Dubna. Preliminary results show a peak at about 2 MeV [13]. If true, this result supports our calculations with the ${}^3\text{H}$ - n interaction from [11]. According to systematics of hydrogen and helium isotopes this result implies that another superheavy isotope ${}^7\text{H}$ could be a slightly unbound state with small width.

We wish to acknowledge the support from the Chalmers University of Technology and the Niels Bohr Institute, where much of this work was carried out. The Royal Swedish Academy of Science and RFBR support from Grant No. 99-02-17610 are acknowledged.

¹Note that the width for the $1/2^+$ state estimated in conventional R -matrix approach for the s -wave decay to the ${}^3\text{H}$ + “dineutron” channel, is about 10–15 MeV. This value should be compared to the 3–4 MeV width from Table I. The reason for this relatively narrow width is a three-body nature of the state.

[1] J. J. Bevelacqua, Nucl. Phys. **A357**, 126 (1981).
 [2] N. A. F. M. Poppelier, L. D. Wood, and P. W. M. Glaudemans, Phys. Lett. **157B**, 120 (1985).
 [3] E. G. Adelberger *et al.*, Phys. Lett. **25B**, 595 (1967).
 [4] K. Seth and B. Parker, Phys. Rev. Lett. **66**, 2448 (1991).
 [5] D. V. Aleksandrov, E. Yu. Nikolsky, B. G. Novatsky, and D. N. Stepanov, Proceedings of the International Conference on Exotic Nuclei and Atomic Mass, Arles, France (1995), p. 329.
 [6] M. G. Gornov *et al.*, Pis'ma Zh. Éksp. Teor. Fiz. **45**, 205 (1987) [JETP Lett. **45**, 252 (1987)].
 [7] M. V. Zhukov *et al.*, Phys. Rep. **231**, 151 (1993).
 [8] B. V. Danilin and M. V. Zhukov, Yad. Fiz. **56**, 67 (1993)

[Phys. At. Nucl. **56**, 460 (1993)]; B. V. Danilin, I. J. Thompson, J. S. Vaagen, and M. V. Zhukov, Nucl. Phys. **A632**, 383 (1998).
 [9] L. V. Grigorenko *et al.*, Phys. Rev. C **57**, R2099 (1998); **60**, 044312 (1999).
 [10] T. A. Tombrello, Phys. Rev. **143**, 143 (1966).
 [11] D. V. Aleksandrov *et al.*, Pis'ma Zh. Éksp. Teor. Fiz. **62**, 18 (1995) [JETP Lett. **62**, 18 (1995)].
 [12] D. Gogny, P. Pires, and R. de Tournel, Phys. Lett. **32B**, 591 (1970).
 [13] A. A. Korshennikov (private communication).